


 Cite this: *RSC Adv.*, 2020, 10, 28755

Synthesis of alginate–polycation capsules of different composition: characterization and their adsorption for [As(III)] and [As(V)] from aqueous solutions

 Cristopeer Thomas-Busani,^a José Andrei Sarabia-Sainz,^b Jaqueline García-Hernández,^c Tomás J. Madera-Santana,^d Luz Vázquez-Moreno^a and Gabriela Ramos-Clamont Montfort^{b*}

The uptake of arsenite [As(III)] and arsenate [As(V)] by functionalized calcium alginate (Ca-Alg) beads from aqueous solutions was investigated. Ca-Alg beads were protonated with poly-L-lysine (PLL) or polyethyleneimine (PEI) using 1-ethyl-3-(3-dimethylaminopropyl)carbodiimide/*N*-hydroxysuccinimide (EDC/NHS) or glutaraldehyde (GA) as crosslinking agents. Four types of protonated beads were prepared: Ca-Alg-EDC/NHS (PLL or PEI) and Ca-Alg-GA (PLL or PEI). Fourier transform infrared spectroscopy in total attenuated reflection mode (FTIR-ATR), analysis showed presence and increased intensity of bands corresponding to OH, NH, CH₂ and CH₃ groups in modifications with both polycations. In addition, thermogravimetric analysis and atomic force microscopy of all modified capsules showed an increase in thermal stability and uniformity of the capsules, respectively. Ca-Alg-EDC/NHS-PLL beads had the maximum adsorption capacity of [As(V)] (312.9 ± 4.7 μg g⁻¹ of the alginate) at pH 7.0 and 15 minute exposure, while Ca-Alg-EDC/NHS-PEI beads had the maximum adsorption capacity of [As(III)] (1052.1 ± 4.6 μg g⁻¹ of alginate). However, all these EDC containing beads were degraded in the presence of citrate. Ca-Alg-GA-PEI beads removed 252.8 ± 9.7 μg of [As(V)] μg g⁻¹ of alginate and 524.7 ± 5.3 de [As(III)] μg g⁻¹ of alginate, resulting the most stable capsules and suitable for As removal.

Received 11th June 2020

Accepted 24th July 2020

DOI: 10.1039/d0ra05135g

rsc.li/rsc-advances

1. Introduction

Arsenic (As) is recognized as a cancer promoter and inducer of a wide range of cancer-independent health risks.¹ Prolonged (chronic) exposure to low concentrations of As can cause skin and nervous system changes, cardiovascular complications, diabetes, as well as cancer of skin, lung, liver, kidney and bladder.² One of the main paths for human arsenic exposure is contaminated drinking water, even at low concentrations of As. Actually, the World Health Organization (WHO) estimates that more than 200 million people around the world drink water with As concentration exceeding 10 μg L⁻¹ which is the

maximum allowed limit.³ This problem is seen as one of the main limitations to safe water supply in the near future.^{3,4}

Arsenic leaches into water bodies from natural deposits or waste generated by anthropogenic activities. The last include mining and metallurgy, industries producing paint and wood preservatives, and the application of persistent arsenic fertilizers (currently prohibited).⁴ The most common As chemical forms in water are arsenate [As(V)] and arsenite [As(III)]. The latter is more toxic, water-soluble, abundant, and difficult to remove.² Biosorption using alginate represents an alternative to removing low concentrations of As (10–100 μg L⁻¹) from drinking water.⁵

Alginate has been shown to be a good adsorbent of heavy metals. This anionic polymer, typically extracted from brown seaweed, is cheap to produce and generally recognized as safe (GRAS).⁶ The crosslinking of alginate with divalent ions such as Ca²⁺ allows the formation of hydrogels with a structure called egg-box. The hydrogel can be synthesized in the form of capsules using the extrusion dripping method.⁷ Nussinovitch and Dagan (ref. 8) used alginate–gellan capsules to remove several heavy ions from solutions and showed high adsorption efficiencies to Pb²⁺, Cu²⁺, Cd²⁺, and Ni²⁺. (316, 219, 197, and 65 mg g⁻¹ of dry alginate, respectively). Calcium alginate beads

^aCoordinación de Ciencia de los Alimentos, Centro de Investigación en Alimentación y Desarrollo A.C., Carretera Gustavo Enrique Astiazarán Rosas, No. 46. Col. La Victoria, C.P. 83304, Hermosillo, Sonora, Mexico. E-mail: gramos@ciad.mx

^bLaboratorio de Biofísica Médica, Departamento de Investigación en Física, Universidad de Sonora, Blvd. Luis Encinas y Rosales. Col. Centro, C.P. 83000, Hermosillo, Sonora, Mexico

^cCoordinación Guaymas, Centro de Investigación en Alimentación y Desarrollo, Sánchez Taboada Carretera al Varadero Nacional km 6.6, Col. Las Playitas, Guaymas, Sector Varadero, Las Playitas, 85480 Heroica Guaymas, Son, Mexico

^dCoordinación de Tecnología de Alimentos de Origen Vegetal, Centro de Investigación en Alimentación y Desarrollo, Carretera Gustavo Enrique Astiazarán Rosas, No. 46. Col. La Victoria, C.P. 83304, Hermosillo, Sonora, Mexico



have also been successfully used to remove Ag^{2+} , Au^{2+} , Cd^{2+} , and Cu^{2+} ions.⁹ In these studies, the biosorption mechanism is based on conventional charge interactions, that is the cation's affinity to negative charged alginate.⁹ This mechanism could not be used for biosorption of [As(III)] and [As(V)] because these ions carry total negative charges. However, an additional advantage of alginate is that the surface of its capsules can be functionalized to acquire new properties and allow new interactions to be established.¹⁰

The protonation of alginate with polycations is possible due to the stability of alginate negative charge over a wide pH range.⁵ This feature allows the formation of complexes with strongly positively charged moiety like ions present in poly-L-lysine (PLL), poly-L-ornithine (PLO), poly-methylene-co-guanidine (PMCG), polyethyleneimine (PEI) and chitosan.¹¹ Formation of positively charged alginate beads comes from electrostatic interactions established between positive polycation groups and alginate carboxyl groups on the outer layer of alginate capsules. These positive particles are more stable, less porous and more biocompatible with the human organism. Thus, they are studied in biomedical applications such as controlled drug release, organ transplantation and tissue engineering.^{12,13} The downfall of these positively charged beads is that they can be destabilized by changes in pH or ionic strength.¹¹

One way to form more stable alginate protonated beads is by the conjugation of polycations with alginate using a crosslinker, for example, 1-ethyl-3-(3-dimethylaminopropyl)carbodiimide (EDC) or glutaraldehyde (GA). These interconnecting agents have been tested in tissue engineering by crisscrossing them with collagen.⁹ Poly-L-lysine (PLL) and polyethyleneimine (PEI) are good candidates for the formation of alginate–polyanion gels due to their low cost and high availability.¹⁴ Alginate–polyethylene network formed using GA as a crosslinker increased the stability of alginate capsules loaded with different microorganisms.¹¹ EDC supported crosslinked alginate with different molecules has been investigated as copper ion removal network, controlled drug release capsules, and tissue engineering scaffolds.^{15,16} The common strategy to synthesize alginate protonated gels is to prepare suspensions of alginate, mix them with the polyanion to start crosslinking reaction and finally add the crosslinking.^{11,15,16}

To properly design alginate–polyanion gel beads for [As(V)] and [As(III)] adsorption, the amino groups of PLL and PEI need to be exposed on the surface of the capsules. The crosslinker EDC reacts with the carboxyl groups of the alginate forming an unstable intermediate. The addition of *N*-hydroxysuccinimide (NHS) stabilizes the system by forming an ester. When the polycations are added to alginate beads, a nucleophilic substitution of type $\text{S}_{\text{N}}2$ is carried out, where the ester is replaced by the amino groups present in the polycations, allowing the formation of a covalent amide-type bond, between the amino groups of polycations and carboxyl groups (mannuronic acid blocks that do not intervene in calcium gelling) of alginate.⁹ Fig. 1A represents a model of this reaction when using PLL or PEI.

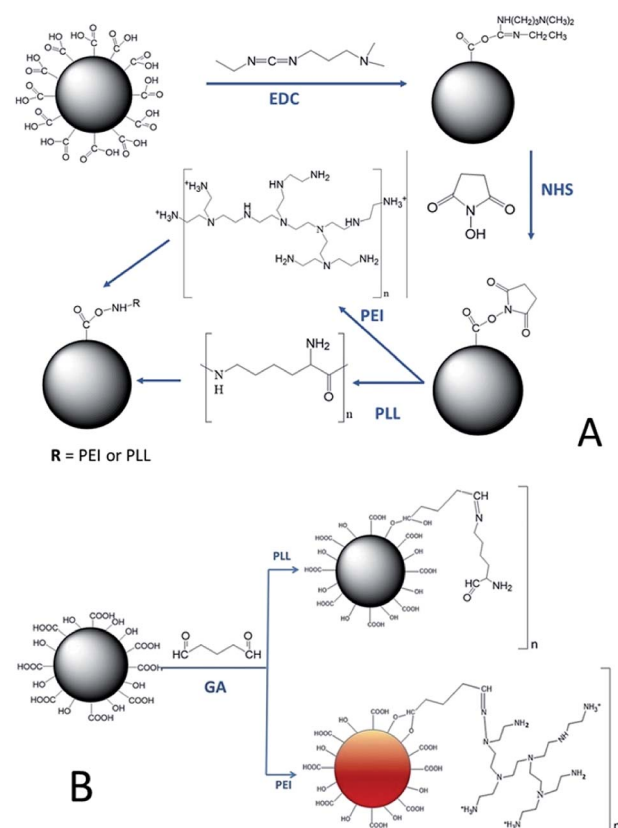


Fig. 1 Model of crosslinking reaction for modification of calcium alginate beads with poly-L-lysine (PLL) or polyethyleneimine (PEI). (A) Crosslinking reaction with 1-ethyl-3-(3-dimethylaminopropyl)carbodiimide/*N*-hydroxysuccinimide (EDC/NHS). (B) Crosslinking with glutaraldehyde (GA).

Fig. 1B shows a model of crosslinking reaction using glutaraldehyde (GA). By submerging alginate capsules into polycation solutions, there are electrostatic interactions with the alginate carboxyl groups, which are unstable. The role of GA is to stabilize such interactions as it can react with both the amino groups of polycations and with the hydroxyl groups of the alginate.¹⁷ This crosslinking prevents polycations from dissociating due to changes in pH or ion strength, by forming covalent bonds of acetal type with hydroxyl and imine bond with amines.¹¹

Therefore, we propose to obtain first the capsules of calcium crosslinked alginate and then treat them with the polycations in the presence of the crosslinkers. After characterization, they were used as bio-sorbent matrices for [As(III)] and [As(V)] in aqueous solution.

2. Materials and methods

2.1 Materials

The food-grade alginate was obtained from Ingredient Solutions Inc. (Waldo, ME, USA). Polyethyleneimine (PEI) (M_w -25 000) and poly-L-lysine (PLL), as well as the rest of the reagents, were purchased from Sigma-Aldrich (St. Louis, MO, USA). All reagents were analytical grade and used as received.



2.2 Synthesis of alginate capsules

The alginate capsules (Ca-Alg) were synthesized by the extrusion method using a B-395 Pro Encapsulator (Buchi Labortechnik AG, Flawil, CHE) and a 750 μm nozzle. An alginate suspension (1% w/v) was pumped through the encapsulator into a hardening solution containing CaCl_2 (0.4 M). The vibration frequency was 350 Hz, the electrode voltage was 1500 V, the pressure of 600–800 mbar. The alginate capsules were left in the hardening solution for 30 min with constant stirring of 150 rpm. Subsequently, the Ca-Alg capsules were washed three times with deionized water to remove calcium that did not react and were kept at 4 $^\circ\text{C}$ until used.

2.3 Protonation of the alginate capsules

Ca-Alg capsules were protonated with PLL or PEI using EDC/NHS or GA as crosslinking agents. For a typical synthesis of Ca-Alg-EDC/NHS capsules (PLL or PEI) 35 mg of EDC was added to every 100 mL of gelled alginate solution (35 g of Ca-Alg capsules) and left to stir at ~ 75 rpm for 1 h at 25 $^\circ\text{C}$. Subsequently, 15 mg of NHS was added and the mixture was left stirring another 1 h. After that time, the capsules were collected and submerged, separately, in 200 mL of PEI solution at 1.5% (w/v) or PLL at 1.5% (v/v), left in agitation for 24 h at 25 $^\circ\text{C}$. The final capsules were collected, washed three times with deionized water to remove PEI or PLL that did not react, and were labelled Ca-Alg-EDC/NHS-PEI and Ca-Alg-EDC/NHS-PLL, respectively. Five batches of each bead type were prepared for the study.

When GA was used as crosslinker, the Ca-Alg beads were first immersed, separately, in 200 mL of PEI solution at 1.5% (w/v) or PLL at 1.5% (v/v) for 24 h at 25 $^\circ\text{C}$. Then, they were collected and immersed in 100 mL of 2% (v/v) GA solution for 1 h. The modified beads were collected, washed three times with deionized water to remove unreacted PEI, PLL, and GA. These samples were labelled as Ca-Alg-GA-PLL and Ca-Alg-GA-PEI.

2.4 Morphology, size and charge

The morphology of the different alginate beads was determined using a Stereomicroscope (Stemi DV4, Carl Zeiss, Gottingen, Germany). Beads were placed on a black background for contrast, and the photographs were recorded at $10\times$ magnification. The diameter of the beads was measured using a digital caliper model 62379-531 (Traceable, Friendswood, TX, USA). 120 capsules of each treatment were measured by sampling 60 capsules at random for each replica. The moisture content was determined in triplicate, using the AOAC standard method # 927.05.¹⁸

Beads surface charge was determined at 25 $^\circ\text{C}$ by measuring their zeta potential (ζ), in a Zetasizer Nano-ZS90 (Malvern Instrument Ltd. Worcestershire, UK). Beads were suspended in deionized water. To assay the effect of the pH of normal drinking water over protonated alginate, ζ of the capsules was determined in a range of 6.0 to 7.5. Measurements were made in triplicate, with 100 runs per replicate. The pH was adjusted with 1 M NaOH and 1 M HCl solutions.

2.5 Infrared spectroscopy with Fourier transform in total attenuated reflection mode (FTIR-ATR)

The spectra of Infrared spectroscopy with Fourier transform in total attenuated reflection mode (FTIR-ATR) were acquired using a Cary 630 Spectrometer (Agilent, Santa Clara, CA, USA). The spectral range analyzed was 4000 to 500 cm^{-1} with 4 cm^{-1} resolution. Sixty four scans were averaged for each spectrum. Analysis of each sample was duplicated.

2.6 Thermogravimetric/derivative thermogravimetry (TGA/DTG) analysis

The thermal stability of the alginate–polyanion capsules was analyzed using a Discovery thermobalance (TA Instrument, New Castle, DE), in a range of 25 $^\circ\text{C}$ to 600 $^\circ\text{C}$ with a heating rate of 10 $^\circ\text{C min}^{-1}$ under nitrogen flow. The initial and final degradation temperatures of the polymer were determined from TGA and DTG curves. The analysis was done in duplicate.

2.7 Atomic force microscopy (AFM)

The topography of the capsules was studied using an XE-Bio Atomic Force Microscope (PARK System, CA) in non-contact mode, with a PPP-NCHR tip and $20 \times 20 \mu\text{m}$ 3D images were built in XEI-AFM (Park System, CA) software. The samples were placed on a slide and allowed to dry for 30 min at room temperature. The analysis was done in duplicate.

2.8 Degradation stability

To determine the stability of degradation, 12 g of capsules of each type were placed in 80 mM solution of sodium citrate for 72 h. Every 6 hours a stereomicroscope observation was made to determine whether the capsules were degraded or if there were changes in the diameter. The experiment was done in duplicate.

2.9 Biosorption tests of arsenate and arsenite in column

The biosorption tests for $[\text{As}(\text{v})]$ and $[\text{As}(\text{iii})]$ were carried out in a fixed column. Capsules (12 g of control or modified) were individually packed into a 12.2 cm \times 2.8 cm glass column, Sigma Aldrich (St. Louis, MO, USA) attached to a Bio-Rad peristaltic pump (Hercules, CA, USA). The adsorption capacity of the alginate–polycation beads was determined by individually passing 15 mL of $[\text{As}(\text{v})]$ or $[\text{As}(\text{iii})]$ with a concentration of 100 $\mu\text{g L}^{-1}$ at a pH of 7.0 ± 0.1 with a flow rate of 1.5 mL min^{-1} , establishing a residence time of 15 min. The experiments were done in triplicate. Quantification of unadsorbed arsenic was carried out by anodic stripping voltammetry supported by a Metrohm 797 VA computer (Herisau, Switzerland).

The removal efficiency was calculated using the following equation:

$$\text{ER} = (C_i - C_f)100/C_i$$

where ER is the removal efficiency (%), C_i and C_f are the initial and final As concentrations, respectively ($\mu\text{g L}^{-1}$).

The maximum adsorption capacity was calculated using the following equation:



$$Q_e = (C_0 - C_e)V/m$$

where Q_e is the maximum adsorption (mg g^{-1}), C_0 and C_e are initial and at the equilibrium concentrations of arsenic, respectively ($\mu\text{g L}^{-1}$), V is the volume of the solution used (mL), and m is the mass (g) of the adsorbent used. The recommendations established for waste management were followed.

2.10 Scanning electron microscope (SEM) and energy dispersive X-ray analysis

Surface morphology and elemental analysis of the Ca-Alg-GA-PEI beads was studied through scanning electron microscope (JEOL (JSM-7600F, Tokyo, Japan) equipped with an EDX detector Oxford INCA energy 200 (Oxford Instruments Analytical, Wycombe, UK), operating at 15 kV for 80 s. Fully dried samples were mounted, and sputter coated with 5 nm of palladium-gold.

2.11 Desorption and reutilization

Desorption analysis were conducted using the same condition for biosorption test in column (Section 2.9). After NaOH (1 mol L^{-1}) was applied to desorb $[\text{As(III)}]$ or $[\text{As(V)}]$ adsorption from Ca-Alg-GA-PEI. Beads were subsequently washed with deionized water until reaching a neutral pH. Then biosorption tests were repeated for a total of five adsorption/desorption cycles. The obtained results were expressed as biosorption capacity. Experiments were conducted in triplicate.

2.12 Statistical analysis

All numerical data were analyzed by NCSS 2007 statistical software (Statistical Analysis and Graphics, Kaysville, UT, USA). Means \pm standard error were calculated for each set of results. For data analysis, a one-way analysis of variance (ANOVA) was performed ($p < 0.05$) and means compared using the Tukey–Kramer test. Graphs were constructed in SigmaPlot software 11.0 (Systat Software Inc, San José, CA, USA).

3. Results and discussion

3.1 Morphology, size, and charge of alginate–polycation capsules

Crosslinking with EDC/NHS did not affect the quasi-spherical shape of alginate beads (Fig. 2A–C). Beads crosslinked with PLL and PEI, using EDC/NHS (Ca-Alg-EDC/NHS-PLL and Ca-Alg-EDC/NHS-PEI), were transparent and with similar sizes to original Ca-Alg capsules. However, the moisture content decreased ($p < 0.05$), possibly due to the increase in solids content (Table 1). As expected, an important modification occurred in the surface charge, which changed from negative ($\sim -27 \text{ mV}$) in Ca-Alg beads to positive ($\sim +23 \text{ mV}$) in beads hardened with PLL or PEI. This charge shift proves the incorporation of polycations to the particle surface.

The GA crosslinked beads (Ca-Alg-GA-PLL and Ca-Alg-GA-PEI) were oval shape (Fig. 2D and E). Also, smaller in size and moisture content ($p < 0.05$) than Ca-Alg capsules (Table 1). When reacting with GA, alginate loses OH groups that can

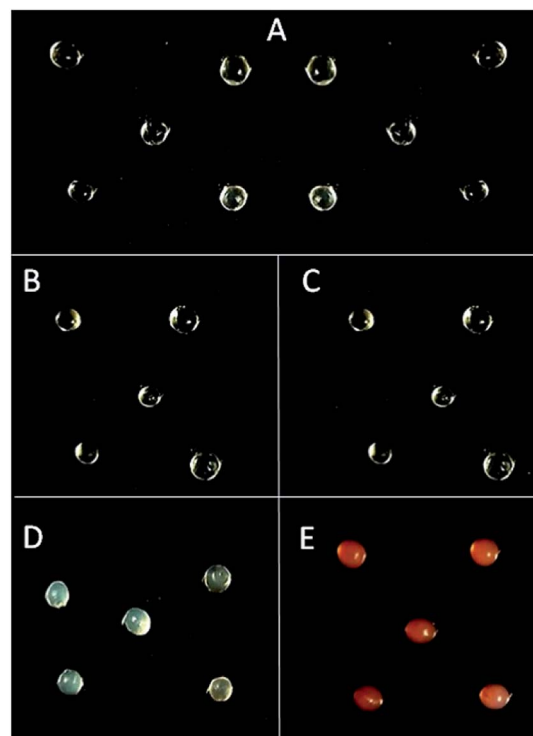


Fig. 2 Morphology of calcium alginate beads (Ca-Alg) protonated with poly-L-lysine (PLL) or polyethyleneimine (PEI). (A) Ca-Alg beads; (B) Ca-Alg-EDC/NHS-PLL; (C) Ca-Alg-EDC/NHS-PEI; (D) Ca-Alg-GA-PLL and (E) Ca-Alg-GA-PEI.

otherwise be available to capture water through the formation of hydrogen bonds.⁹ In addition, during the reaction of the amine from polycation (nucleophilic) with the carbonyl (electrophile) of the GA, a hemiaminal intermediary ($\text{NH-CR}_2\text{-OH}$) is formed, followed by the loss of water during the formation of the imine bond (C=N). These processes produce slight dehydration of the capsules.^{19,20} The surface charge of the Ca-Alg-PLL-GA and Ca-Alg-PEI-GA beads had positive values ($+0.6273 \pm 0.12 \text{ mV}$ and $+10.29 \pm 0.16$, respectively). Furthermore, the positive surface charge was greater ($P < 0.05$) when using EDC/NHS than GA as a crosslinker (Table 1). This may be due to the type of cross-connection formed, as carbodiimide increases amines exposure to the polycation.

In contrast to EDC/NHS formed capsules, both types of GA hardened capsules were opaque. In addition, Ca-Alg-GA-PEI capsules gained a red color (Fig. 2E). The red color is an indication of the formation of unsaturated alternating imine-type bonds resulting from the reaction between GA and PEI.²¹ The lack of red color in Ca-Alg-GA-PLL capsules is possibly due to a lower degree of crosslinking between PLL and GA than between PEI and GA since PLL molecule has fewer amino groups than PEI molecule.⁹

The pH changes, within the studied range (6.0–7.5), had no effect ($p > 0.05$) on the surface charge of any of the modified capsules, PEI nor PLL (data not shown). This stability confirms that both the PEI amino groups, as well as those of PLL,



Table 1 Characterization of calcium alginate beads before and after protonation with poly-L-lysine (PLL) or polyethyleneimine (PEI)^a

Treatment	Size (mm)	Moisture content (%)	Z potential (mV)
Ca-Alg (control)	1.27 ± 0.09 ^a	96.14 ± 0.4 ^a	-27.5 ± 1.46 ^a
Ca-Alg-EDC/NHS-PLL	1.27 ± 0.13 ^a	92.92 ± 0.13 ^b	+23.6 ± 0.15 ^c
Ca-Alg-EDC/NHS-PEI	1.26 ± 0.19 ^a	93.32 ± 0.05 ^b	+23.3 ± 0.27 ^c
Ca-Alg-GA-PLL	1.23 ± 0.11 ^b	90.26 ± 0.63 ^c	+0.64 ± 0.12 ^d
Ca-Alg-GA-PEI	1.20 ± 0.11 ^c	82.14 ± 1.04 ^d	+10.3 ± 0.16 ^c

^a Ca-Alg: calcium alginate beads. Crosslinking agents EDC/NHS: 1-ethyl-3-(3-dimethylaminopropyl)carbodiimide/*N*-hydroxysuccinimide; GA: glutaraldehyde. Values are expressed as means ± standard error. Different letters in the same column denote a statistical difference ($p < 0.05$).

remained protonated at the pH commonly found in drinking water.²²

3.2 FTIR-ATR analysis

FTIR-ATR was used to recognize interactions between the alginate matrix and polycations. All spectrum were normalized with the band situated at 1415 cm⁻¹. Fig. 3A compares the FTIR-ATR absorbance spectra of Ca-Alg beads and those modified with PLL. Ca-Alg capsules presented the characteristic spectrum of alginate with a wide peak centred at approximately 3300 cm⁻¹ indicating the stretching vibrations of OH groups. Also, low-intensity bands located approximately at 2933 cm⁻¹, which

are attributed to C-H stretching vibration, two peaks about 1593 cm⁻¹ and 1415 cm⁻¹ due to the asymmetrical and symmetrical signals of the COO-groups, respectively. The peaks observed in the region between 950 and 1200 cm⁻¹ correspond to various vibrations in the carbohydrate rings. Specifically, the peak at 1029 cm⁻¹ is assigned to the glycosidic (C-O-C) bonds of the polymer.¹⁴

The crosslinking of the alginate with PLL using EDC/NHS modified the bands corresponding to the stretching of the OH groups of the alginate at 3334 cm⁻¹ (Fig. 3A). An increase in peak intensity and the appearance of two small, new bands at 3348 cm⁻¹ and 3237 cm⁻¹ coincide with amide A region thus indicating the formation of amide-type covalent bonds between the amino groups of the PLL and the carboxyl groups of alginate.⁹ The signal corresponding to the COO-asymmetrical groups in the Ca-Alg capsules (1593 cm⁻¹) appeared as a higher intensity band in the Alg-EDC/NHS-PLL capsules. In addition, there was a slight displacement to 1608 cm⁻¹ possibly due to the interactions between the carbonyl of alginate and the amine of PLL. These changes are indications of the interaction of the COO-groups of the alginate with the NH₂ groups of the PLL.¹⁴

The crosslinking with PLL using GA showed as an increase in the intensities of the bands corresponding to the methylene groups, attributed to the presence of these groups in the lateral chains of the PLL incorporated on the surface of the alginate beads. In addition, the appearance of a small band at 1697 cm⁻¹ was observed that can be attributed to the bending of the amino groups present in the PLL attached to the alginate matrix. The band at 822 cm⁻¹ shifted to 805 cm⁻¹ which is an indication of the incorporation of the PLL to the alginate.²³

The crosslinking of alginate with PEI using EDC/NHS was characterized by a broad band at 3148 cm⁻¹, attributed to the OH groups of alginate and NH of PEI (Fig. 3B). Besides, two small bands appeared at 3341 and 3267 cm⁻¹, assigned to the PEI amino groups attached to the alginate matrix. The peaks at 2911 and 2807 cm⁻¹ corresponding to C-H stretch of CH₂ and CH₃ groups significantly increased their intensity due to the incorporation of PEI methylene groups at the surface of alginate capsules.²⁴ The signal corresponding to the COO-asymmetrical bend in the Ca-Alg capsules (1593 cm⁻¹) shifted to 1585 cm⁻¹, due to interactions with the amino groups of the PEI. The band at 1029 cm⁻¹, (C-O-C and/or C-N), also showed a slight displacement (1022 cm⁻¹). The band at 881 cm⁻¹ which

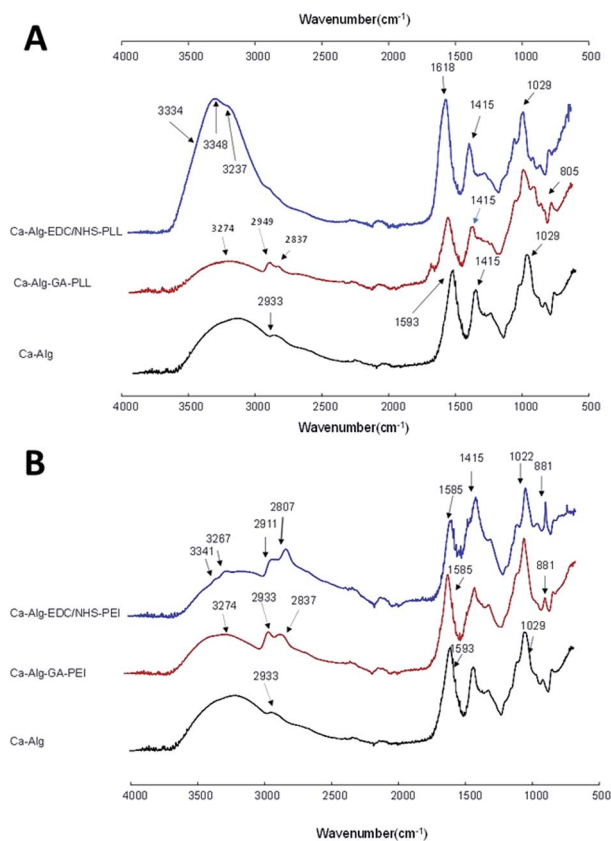


Fig. 3 Attenuated total reflectance Fourier transform infrared spectroscopy for calcium alginate beads functionalized with (A) poly-L-lysine and (B) polyethyleneimine.



corresponds to the signal of the primary amines, proves the amine group presence into the alginate capsules.²³

In the spectra of Ca-Alg-PEI capsules crosslinked with GA, an increase in the intensity of the OH group band (3274 cm^{-1}) is well visible due to the presence of NH groups from PEI. Unlike in crosslinking with EDC/NHS, bands in 3341 and 3267 cm^{-1} did not appear, because covalent links between alginate and PEI are not formed in the same manner. However, the intensity of the peak at 2933 cm^{-1} increased and a band at 2837 cm^{-1} appeared due to additional CH_2 and CH_3 groups from the PEI polymer. The peak at 1593 cm^{-1} shifted to 1585 cm^{-1} attributed to the formation of imine bonds between GA aldehyde and PEI amine group, confirming covalent bonding of the polycation coating to the alginate matrix.²⁴ The measured wavenumbers of the bands before and after the modification are summarized in Table 2.

3.3 Thermogravimetric/derivative thermogravimetry (TGA/DTG) analysis

Fig. 4 shows the thermograph curves of the modified alginate capsules with PLL (A) and their derivatives (B). The thermograms of neat Ca-Alg, had a single-stage decomposition which occurs between $33\text{ }^\circ\text{C}$ and $130\text{ }^\circ\text{C}$, with a maximum of degradation at $111\text{ }^\circ\text{C}$. The slow drop of the mass loss is attributed to the loss of moisture and the degradation of the alginate chains caused by heating.²⁵

The thermogram of the Ca-Alg-EDC/NHS-PLL capsules showed a degradation process in two stages. The first stage began at $33\text{ }^\circ\text{C}$ and ended at $107\text{ }^\circ\text{C}$, with a maximum degradation occurring at $84\text{ }^\circ\text{C}$. This step represents moisture loss and degradation of alginate. The second degradation occurred between $199\text{ }^\circ\text{C}$ and $496\text{ }^\circ\text{C}$, with a maximum degradation at $201\text{ }^\circ\text{C}$. This degradation can be attributed to the decomposition of the polyamine acid. Similar patterns of lysine and arginine decomposition was reported by Zhang *et al.*²² Ca-Alg-PEI capsules crosslinked with GA showed a one-step degradation starting at $49\text{ }^\circ\text{C}$ and ending at $182\text{ }^\circ\text{C}$, with a maximum

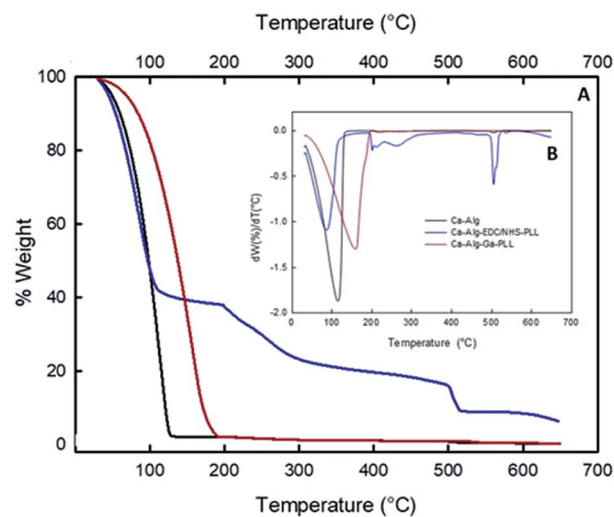


Fig. 4 Thermogravimetric/derivative thermogravimetry analysis for calcium alginate beads functionalized with poly-L-lysine (PLL). Crosslinking agents EDC/NHS: 1-ethyl-3-(3-dimethylaminopropyl) carbodiimide/*N*-hydroxysuccinimide; GA: glutaraldehyde.

degradation at $168\text{ }^\circ\text{C}$. This increase in the thermal stability of alginate beads is due to the matrix and polycation interactions forming a harder network. Similar behaviour was reported by Poon *et al.*²⁰ in chitosan copolymers.

Fig. 5 shows the thermograph curves of PEI-modified alginate capsules (A) and their derivatives (B). The thermograph of Ca-Alg-EDC/NHS-PEI capsules had a one-stage decomposition, similar to Ca-Alg capsules. However, the initial degradation and maximum degradation temperatures increased from $33\text{ }^\circ\text{C}$ to $46\text{ }^\circ\text{C}$ and from $111\text{ }^\circ\text{C}$ to $153\text{ }^\circ\text{C}$, respectively. These thermal shifts indicate greater thermal stability of the capsules due to

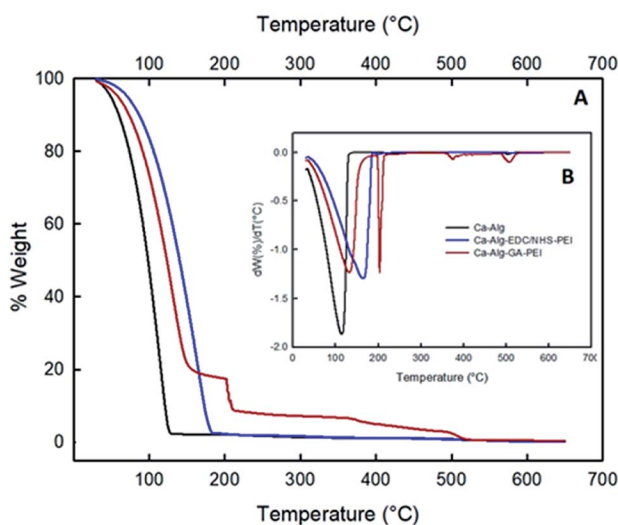


Fig. 5 Thermogravimetric/derivative thermogravimetry analysis for calcium alginate beads functionalized with polyethyleneimine (PEI). Crosslinking agents EDC/NHS: 1-ethyl-3-(3-dimethylaminopropyl) carbodiimide/*N*-hydroxysuccinimide; GA: glutaraldehyde.

Table 2 Attenuated total reflectance Fourier transform infrared spectroscopy frequency assignments for protonated calcium alginates beads with poly-L-lysine (PLL) or polyethyleneimine (PEI)^a

Ca-Alg	Ca-Alg-EDC/NHS		Ca-Alg-GA		Assignment
	PLL	PEI	PLL	PEI	
3300	3334	3148	3274	3274	$\nu(\text{OH})$
—	3348; 3237	3341; 3267	3274	3274	$\nu(\text{N-H})$
2933	2933	2911; 2807	2949	2933; 2837	$\nu(\text{C-H})$
—	—	—	1697	—	$\nu(\text{N-H})$
1593	1618	1585	—	1585	$\nu_{\text{a}}(\text{COO}^-)$
1415	1415	1415	1415	1415	$\nu_{\text{s}}(\text{COO}^-)$
1029	1029	1022	1029	1022	$\nu(\text{C-O-C})$
—	822	881	805	881	$\nu(\text{N-H})$

^a Ca-Alg: calcium alginate beads. Crosslinking agents EDC/NHS: 1-ethyl-3-(3-dimethylaminopropyl)carbodiimide/*N*-hydroxysuccinimide; GA: glutaraldehyde. ν : stretching; a: asymmetric; s: symmetric.



formations of a stable crosslinked network between the alginate matrix and the PEI groups.²⁶

Crosslinking PEI using GA presented changes in its decomposition pattern again showing thermal degradation in several stages. The first, between 43 °C and 195 °C, with a maximum degradation at 128 °C can be attributed to the loss of moisture and thermal degradation of alginate.

The second degradation occurred between 198 °C and 368 °C, with a maximum decomposition at 205 °C can be assigned to the breakdown of glutaraldehyde, which occurs very quickly.²⁷ The final stage occurs between 361 °C and 496 °C and can be recognized as the degradation of PEI, with a maximum degradation at 377 °C.¹⁷ Overall, the thermographs of the modified alginate capsules with PLL or PEI, using EDC/NHS or GA as crosslinkers showed an improvement in thermal stability, compared to uncross linked Ca-Alg capsules. This improvement in thermal stability can be explained by the decrease in the mobility of the alginate molecules due to their connection to polycation PLL or PEI. Also, the presence of polycations protects the surface of the capsules exposed to heat and decreases mass loss during thermal decomposition of the sample.²⁶

3.4 Atomic force microscopy (AFM)

The topography of the alginate capsules before and after modification with the polycations was analyzed using atomic force microscopy. The root mean square roughness (R_q) was measured for 20 by 20 μm areas for all samples. Ca-Alg capsules (Fig. 6A) had a roughness of 313.736 nm with a maximum height of 974.02 nm, an average height of 65.49 nm and a minimum height of 843.04 nm. Capsules crosslinked with PLL (Fig. 6B and C) and PEI (Fig. 6E and F) were more homogeneous and had less rough surfaces. The R_q of all these capsules was

lower than that of Ca-Alg capsules. Xu *et al.*²⁸ coated polyacrylonitrile particles with branched and high molecular weight polycations, and observed a lower surface roughness by increasing the molecular weight of polycations. In short, the results of AFM analysis are further evidence of polycations coating of Ca-Alg capsules.

3.5 Degradation stability

To determine the stability to degradation, the capsules were exposed to sodium citrate solution for 72 h. Ca-Alg capsules degraded during the first 2 hours of sodium citrate exposure while Ca-Alg-EDC/NHS capsules (PLL or PEI) degraded after 24 h, indicating that initial calcium crosslinking is important but not sufficient for the stability. Ca-Alg-GA capsules (PLL or PEI) retained their diameter for the 72 h of treatment. This may be due to the core-like arrangement produced by the GA. No degradation was observed in Ca-Alg-GA-PEI after 120 days of treatment.

3.6 Biosorption of [As(v)] and [As(III)] with protonated alginate capsules

The removal efficiency and the maximum adsorption capacity of the alginate–polyanion beads were determined using aqueous solutions of [As(v)] and [As(III)] at 100 $\mu\text{g L}^{-1}$ and pH 7.0 \pm 0.1. Ca-Alg-GA-PEI capsules had the highest efficiency (37.9 \pm 1.0%) to adsorb arsenate (Table 3). The highest maximum adsorption capacity per gram of dry alginate was recorded for Ca-Alg-EDC/NHS-PLL capsules (312.9 \pm 4.7 $\mu\text{g g}^{-1}$ of alginate). At pH equal 7.0, the predominant species with pentavalent arsenic, [As(v)], is $\text{H}_2\text{AsO}_4^{2-}$. It is believed that the uptake of [As(v)] ions occurs through electrostatic interactions between the negative arsenate and the protonated amino groups of the polycation. This process requires two binding sites in the adsorbent. Greater removal of [As(v)] can be achieved at acid pH conditions, where the amino groups have the highest concentration of positive charges.²⁹ However, decreasing the pH of drinking water is not an effective method. Several authors have studied the removal of [As(v)] at near-neutral pH. Sigdel *et al.*³⁰ used iron-impregnated alginate capsules and managed to remove 30% of the [As(v)] in aqueous solution at pH 6.0. Li *et al.*³¹ achieved sorption of 55% of [As(v)] at pH 7.0, using cerium oxide nanoparticles. Raj *et al.*³² used industrial corn waste to remove [As(v)] from aqueous solutions at pH 7.5. The authors found that by crosslinking *Zea mays* cob powder with PEI the adsorption efficiency increased by 12%.

Ca-Alg-GA-PEI beads were also most efficient (69.9 \pm 0.7%) in arsenite adsorption (Table 3), while Ca-Alg-EDC/NHS-PEI capsules showed the maximum adsorption per g capacity of dry alginate (1052.1 \pm 4.6 $\mu\text{g g}^{-1}$ of dry alginate). At pH 7.0 the predominant species of [As(III)] is arsenous acid (H_3AsO_3), which is neutral in a wide range of pH (from 2 to 9.2).³¹ It has been suggested that the main adsorption mechanism for this form of arsenic species is chelation of [As(III)] ions by the functional groups of the adsorbent. The [As(III)] behaves like a Lewis acid with an incomplete octet and is able to capture free electrons. On the other hand, the amino groups present of the

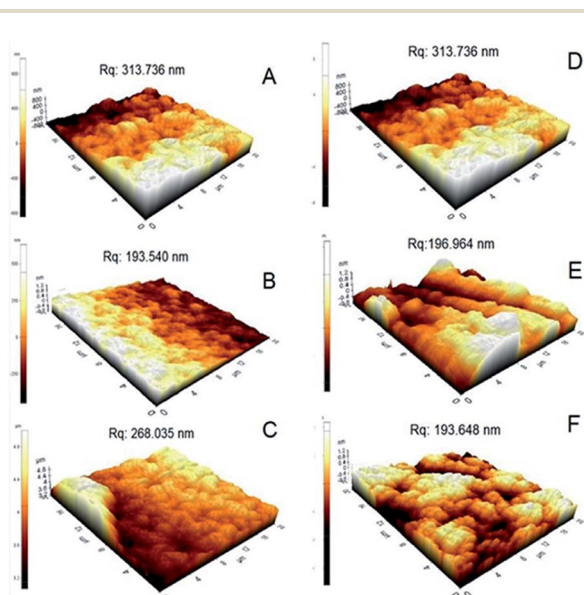


Fig. 6 Atomic force microscopy images topography of calcium alginate beads before (A and D) and after modification with poly-L-lysine: (B) Ca-Alg-EDC/NHS-PLL and (C) Ca-Alg-GA-PLL B or polyethyleneimine (E) Ca-Alg-EDC/NHS-PEI and (F) Ca-Alg-GA-PEI.



Table 3 Arsenate As(v) and arsenite As(III) removal efficiencies and biosorption capacities of protonated calcium alginate (Ca-Alg) beads with poly-L-lysine (PLL) or polyethyleneimine (PEI)^a

Formulation	As(v)		As(III)	
	Removal efficiency (%)	Biosorption capacity ($\mu\text{g g}^{-1}$)	Removal efficiency (%)	Biosorption capacity ($\mu\text{g g}^{-1}$)
Ca-Alg (control)	$0.38 \pm 0.0^{\text{d}}$	$11.7 \pm 1.1^{\text{d}}$	$0.8 \pm 0.1^{\text{c}}$	$21.3 \pm 1.7^{\text{d}}$
Ca-Alg-EDC/NHS-PLL	$17.3 \pm 0.1^{\text{b}}$	$312.9 \pm 4.7^{\text{a}}$	$25.2 \pm 0.4^{\text{d}}$	$448.5 \pm 5.6^{\text{c}}$
Ca-Alg-EDC/NHS-PEI	$14.0 \pm 0.6^{\text{c}}$	$249.6 \pm 12.2^{\text{b}}$	$58.9 \pm 0.4^{\text{b}}$	$1052.1 \pm 4.6^{\text{a}}$
Ca-Alg-GA-PLL	$12.2 \pm 0.4^{\text{c}}$	$152.6 \pm 0.6^{\text{c}}$	$36.7 \pm 0.3^{\text{c}}$	$458.4 \pm 4.3^{\text{c}}$
Ca-Alg-GA-PEI	$37.9 \pm 1.0^{\text{a}}$	$252.8 \pm 9.7^{\text{b}}$	$69.9 \pm 0.7^{\text{a}}$	$524.7 \pm 5.3^{\text{b}}$

^a Ca-Alg: calcium alginate beads. Crosslinking agents EDC/NHS: 1-ethyl-3-(3-dimethylaminopropyl)carbodiimide/*N*-hydroxysuccinimide; GA: glutaraldehyde. Values are expressed as means \pm standard error. Different letters in the same column denote a statistical difference ($p < 0.05$).

alginate–polycation capsules, behave like Lewis bases, donating free electrons, forming the chelate complexes *via* one of the two-bonded ligands.³³

Most treatments designed to remove As from water focus on the removal of [As(v)] but fail or ignore to eliminate [As(III)]. One of the strategies for the elimination of [As(III)] is to oxidize it to [As(v)] using pre-treatment with chlorine or permanganate. During As adsorption, a non-redox-sensitive sorbent such as MnO₂ can also be used to transform [As(III)] into [As(v)] without requiring pretreatment.³⁴ However, some substances present in water may interfere with this oxidation.⁵ Shakoor *et al.*³⁵ studied several biosensors for the removal of [As(III)] and [As(v)] at pH of 7.0. They found that eggshells and plum pits were able to remove 85% and 67% of the [As(III)] respectively after 2 hours of contact. However, the pH had to be reduced to 4.5 in order to adsorb [As(v)]. CuO-functionalized graphene/carbon NTs (CuO-CNTs) were able to remove 2.3 mg g⁻¹ of [As(III)] and 2.4 mg g⁻¹ of [As(v)] at pH of 7 and 5, respectively (contact times of 60 min and 40 min, respectively).³⁶ Although the alginate–polyanion capsules synthesized in this study showed lower adsorption capabilities (Table 3), have the advantage of removing an acceptable amount of [As(III)] and [As(v)] in short contact times and without pH modification.

3.7 SEM-EDX analysis

Ca-Alg-GA-PEI beads were chosen to continue the study due to their high stability. Fig. 7 presents the SEM-EDX analysis for Ca-Alg and Ca-Alg-GA-PEI. EDX assay confirmed the incorporation of nitrogen after the crosslinking of PEI with GA (Fig. 7B) and the incorporation of arsenic in Ca-Alg-GA-PEI beads after adsorption of arsenite (Fig. 7C) or arsenate (Fig. 7D). SEM micrographs showed more cracked surfaces after contact of Ca-Alg-GA-PEI beads with arsenic (Fig. 7C and D). This effect has been attributed to the capture of heavy metals on the sorbent's surface.

3.8 Biosorption mechanism

Ca-Alg-GA-PEI beads were formed *via* PEI grafting onto Ca-Alg beads which creates a considerable number of binding sites (*e.g.* NH³⁺ and NH₂ groups). Fig. 8 compares the FTIR-ATR

absorbance spectra of Ca-Alg-GA-PEI beads before and after [As(III)] and [As(v)] adsorption. Major differences were found in the regions 3700 to 2837 cm⁻¹ and 1720–880 cm⁻¹ indicating [As(III)] or [As(v)] binding to the Ca-Alg-GA-PEI beads. An increase in the peak at 3274 cm⁻¹ after [As(III)] or [As(v)] column application suggests the interaction of both As species with N–H amino groups from PEI. The peak originally at 1585 cm⁻¹ was increased and shifted to 1608 cm⁻¹ suggesting interactions with PEI amino groups coupled with GA–alginate matrix.

In groundwater inorganic oxyanions such as trivalent arsenite [As(III)] and pentavalent arsenate [As(v)] are the predominant As species.⁵ In this aqueous environment the adsorption of [As(III)] and [As(v)] is mainly governed by the pH because it regulates the ionic characteristics of both species as well as the surface properties of the sorption matrix. At pH 7 [As(III)] is mostly in its neutral form (H₃AsO₃ = H₂AsO₃⁻ + H⁺, pK_{a1} = 9.2)

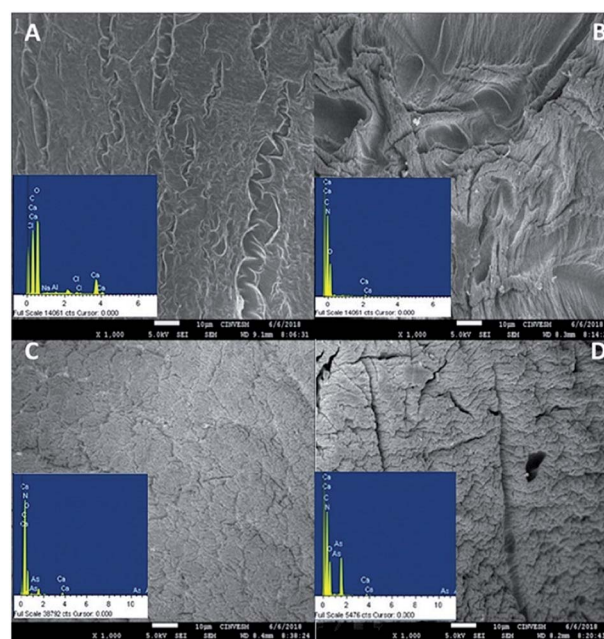


Fig. 7 EDX in SEM images of (A) calcium alginate beads; (B) Ca-Alg-GA-PEI beads; (C) Ca-Alg-GA-PEI beads after biosorption of [As(III)]; (D) Ca-Alg-GA-PEI beads after biosorption of [As(v)].



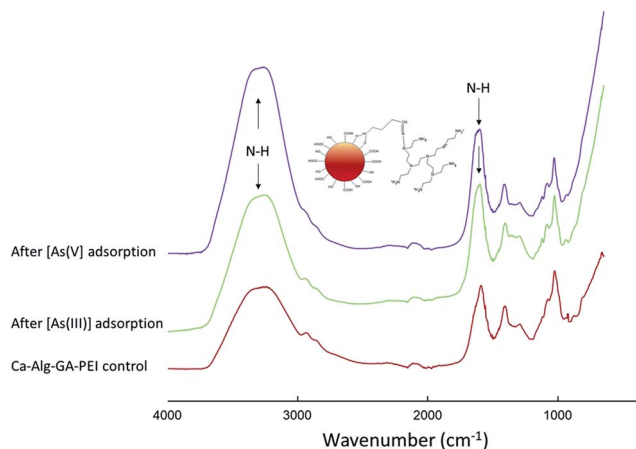


Fig. 8 Attenuated total reflectance Fourier transform infrared spectroscopy for Ca-Alg-GA-PEI beads before and after [As(III)] or [As(V)] adsorption.

and approximately 50% of amino groups remain unprotonated.^{5,37–39} In this context [As(III)] uptake by Ca-Alg-GA-PEI beads is determined by surface complexation of H_3AsO_3 with NH_2 groups.³⁷ This is in agreement with the observations of Daikopoulos *et al.*³⁹ who synthesized amine-rich graphitic carbon nitride for arsenite remediation.

Arsenite biosorption capacity of Ca-Alg-EDC/NHS-PEI beads was higher ($1052.1 \pm 4.6 \mu\text{g g}^{-1}$) than that of Ca-Alg-GA-PEI ones ($524.7 \pm 5.3 \mu\text{g g}^{-1}$) (Table 3). The crosslinker EDC reacts with the carboxyl groups of the alginate forming an unstable intermediate (Fig. 1). The addition of *N*-hydroxysuccinimide (NHS) stabilizes the system by forming an ester, then the ester is replaced by the amino groups present PEI, allowing the formation of a covalent amide-type bond, between the amino groups of polycations and carboxyl groups (mannuronic acid blocks that do not intervene in calcium gelling) of alginate.⁹ On the contrary GA reacts with the amino groups of PEI and the hydroxyl groups of the alginate.¹⁷

This type of reaction allows a greater crosslinking between the alginate and PEI both on the bead surface and within the supporting alginate matrix forming a 3D network that increase the bead stability but also the [As(III)] binding sites with the free amino groups that did not react with GA.⁴⁰ Then excessive crosslinking can adversely affect the binding capacity of the matrix as it seems to have happened with Ca-Alg-GA-PEI. Subsequent experiments should be conducted testing different concentrations of GA in order to find a more adequate balance between crosslinking and available binding sites.

Ca-Alg-EDC/NHS-PLL and Ca-Alg-GA-PLL presented lower biosorption capacities for [As(III)] ($p < 0.05$) than the matrices cross-linked with PEI. This may be because PLL has fewer amino groups than PEI and therefore fewer junction points for arsenite. The biosorption capacities of both (Ca-Alg-EDC/NHS-PLL and Ca-Alg-GA-PLL) were similar to each other ($448.5 \pm 5.6 \mu\text{g g}^{-1}$ and $458.4 \pm 4.3 \mu\text{g g}^{-1}$, respectively), which is an indication of a lower crosslinking of PLL with GA. This can be seen with the naked eye by comparing the colors of Ca-Alg-GA-

PLL (opaque white) and Ca-Alg-GA-PEI (reddish orange) (Fig. 2). The reaction between GA and amines produces compounds with yellow to orange colorations.²¹ Both Ca-Alg-EDC/NHS-PLL and Ca-Alg-GA-PLL showed low stability, so more research should be done on how to improve them.

At pH 7.0 about half of the surface amino groups are protonated and H_2AsO_4^- and HASO_4^{2-} are predicted to appear.^{5,38} Under such a condition, [As(v)] is readily retained by the Ca-Alg-GA-PEI beads *via* electrostatic interaction. Fig. 9 presents the interactions of oxyanions of [As(III)] and [As(v)] with PEI amine groups.

Ca-Alg-EDC/NHS-PLL showed higher [As(v)] adsorption capacity compared to the other matrices (Table 3), this correlates with its net surface charge of $+23.6 \pm 0.15 \text{ mV}$ (Table 1). Ca-Alg-EDC/NHS-PEI showed similar values of net surface charge but lower biosorption capacity than Ca-Alg-EDC/NHS-PLL. This results may be due to the cross-linking of the amino groups with GA. Ca-Alg-GA-PEI showed an [As(v)] uptake similar to Ca-Alg-EDC/NHS-PEI ($252.8 \pm 9.7 \mu\text{g g}^{-1}$ and $249.6 \pm 12.2 \mu\text{g g}^{-1}$, respectively), despite the fact that Ca-Alg-GA-PEI showed a surface charge of $+10.3 \pm 0.16 \text{ mV}$ (Table 1). This may indicate that [As(v)] was retained not only in the surface but also within the supporting bead matrix. This is possible due to the ability of GA to react with the OH groups of the alginate and the amino groups of PEI or PLL and also explains why the Ca-Alg-GA-PLL beds were able to capture [As(v)] even though they showed a surface charge of $+0.64 \pm 0.12 \text{ mV}$ (Table 3).

A very nominal decrease in [As(III)] and [As(v)] removal capacity in five consecutive cycles of sorption/adsorption demonstrates the reusability of Ca-Alg-GA-PEI (Fig. 10). A 9% of arsenate decrease was observed until the fifth sorption/adsorption cycle.

Arsenic adsorption strongly depends of water pH. The range of effective adsorption of both [As(III)] (H_2AsO_3) and [As(v)] (H_2AsO_4^- and HASO_4^{2-}) occurs between a water pH of 6.0 to 7.5. More acidic conditions will increase the adsorption of [As(v)] while more alkaline conditions will increase the adsorption of [As(III)].⁵ At pH of 7.0, Ca-Alg-GA-PEI beads adsorbed both [As(III)] and [As(v)]. This could represent an advantage for water treatment. However, subsequent isotherms, kinetics and thermodynamic studies must be conducted in order to establish the matrix behavior at different pH, redox potential and different sorbent, sorbate and arsenic oxyanions concentrations. Such

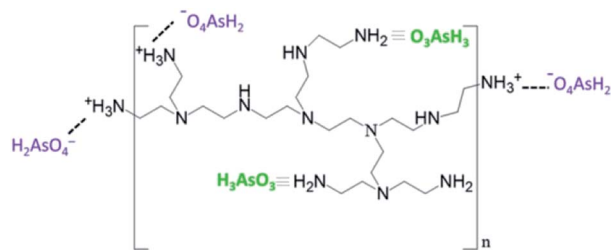


Fig. 9 Schematic representation of the complex interactions of [As(III)] and electrostatic interaction of [As(v)] with Ca-Alg-GA-PEI amine groups.



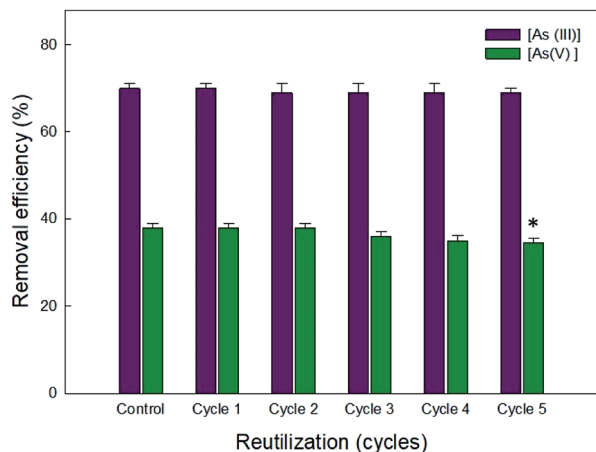


Fig. 10 Removal efficiency of Ca-Alg-GA-PEI after five desorption/adsorption cycles. Asterisk denotes significant difference ($p < 0.05$) between the cycles of the same oxyanion.

studies will provide more accurate information aimed at improving the optimal conditions of use for Ca-Alg-GA-PEI for As removal at specific conditions.

4. Conclusions

The crosslinking agents EDC/NHS and GA were effective in modifying Ca-Alg functionalizing them with PLL or PEI. This modification of the surface capsules allowed the removal of both [As(v)] and [As(III)] oxyanions from neutral water and short contact times of 15 min. At pH 7.0 the proposed adsorption mechanism involves establishing complexes between arsenate and NH_2 and establishing electrostatic interactions between arsenate and NH_3^{3+} groups. Crosslinking with EDC/NHS had greater removal capacity of [As(III)] and [As(v)] than when GA was used. However, they degraded in the presence of calcium citrate, while capsules modified using GA-PEI modification remained stable. The results in the [As(III)] removal (found in its uncharged form at natural water pH) without pre-treatment or pH change has a potential for further applications and advantage over oxidative treatment and conventional techniques of the arsenic removal. However, subsequent isotherms, kinetics and thermodynamic studies must be conducted aimed at optimizing the use of the functionalized matrix in water specific environmental conditions.

Funding

This research was funded by the Consejo Nacional de Ciencia y Tecnología de México (CONACYT), grant number CB169358.

Conflicts of interest

There are no conflict of interest to declare.

Acknowledgements

We are grateful to the Consejo Nacional de Ciencia y Tecnología de México, CONACYT, for the financial support for this research, under project CB169358, as well as for the scholarship awarded for MSc studies. The authors would like to thank to National Laboratory of Nano and Biomaterials (LANNBIO) CINVESTAV-IPN Unidad Mérida (projects FOMIX-Yucatán 2008-108160; CONACYT LAB 2009-01-123913, 292692 y 294643) and to Institutional Analytical Platform of CIAD (PAI-10363) for their analytical facilities, and to Rosa Idalia Armenta Corral for her technical assistance.

References

- 1 W. IARC, available from monographs, <http://www.iarc.fr/ENG/Classification>, 2017.
- 2 M. Jaishankar, T. Tseten, N. Anbalagan, B. B. Mathew and K. N. Beeregowda, *Interdiscip. Toxicol.*, 2014, 7, 60–72.
- 3 World Health Organization Journal, <http://www.who.int/mediacentre/factsheets/fs372/2012>.
- 4 J.-Y. Chung, S.-D. Yu and Y.-S. Hong, *J. Prev. Med. Public Health*, 2014, 47, 253–257.
- 5 N. R. Nicomel, K. Leus, K. Folens, P. Van Der Voort and G. Du Laing, *Int. J. Environ. Res. Public Health*, 2015, 13(1), DOI: 10.3390/ijerph13010062.
- 6 A. K. Zeraatkar, H. Ahmadzadeh, A. F. Talebi, N. R. Moheimani and M. P. McHenry, *J. Environ. Manage.*, 2016, 181, 817–831.
- 7 X. He, Y. Liu, H. Li and H. Li, *RSC Adv.*, 2016, 6, 114779–114782.
- 8 A. Nussinovitch and O. Dagan, *J. Hazard. Mater.*, 2015, 299, 122–131.
- 9 S. Gao, Z. Yuan, W. Guo, M. Chen, S. Liu, T. Xi and Q. Guo, *Mater. Sci. Eng., C*, 2017, 71, 891–900.
- 10 D. Kumar, L. Pandey and J. P. Gaur, *Algal Res.*, 2016, 18, 95–109.
- 11 G. Simó, E. Fernández-Fernández, J. Vila-Crespo, V. Ruipérez and J. M. Rodríguez-Nogales, *Carbohydr. Polym.*, 2017, 170, 1–14.
- 12 L. Baruch and M. Machluf, *Biopolymers*, 2006, 82, 570–579.
- 13 T. Haque, H. Chen, W. Ouyang, C. Martoni, B. Lawuyi, A. M. Urbanska and S. Prakash, *Biotechnol. Lett.*, 2005, 27, 317–322.
- 14 S. K. Tam, J. Dusseault, S. Polizu, M. Menard, J. P. Halle and L. Yahia, *Biomaterials*, 2005, 26, 6950–6961.
- 15 I. P. S. Fernando, D. Kim, J.-W. Nah and Y.-J. Jeon, *Chem. Eng. J.*, 2019, 355, 33–48.
- 16 M. Wang, Q. Yang, X. Zhao and Z. Wang, *Int. J. Biol. Macromol.*, 2019, 138, 1079–1086.
- 17 X. Sun, L. Yang, Q. Li, Z. Liu, T. Dong and H. Liu, *Chem. Eng. J.*, 2015, 262, 101–108.
- 18 W. Horwitz and G. W. Latimer, *Official Methods of Analysis of AOAC International*, AOAC International, Gaithersburg, MD, 2010.
- 19 S. Nagireddi, V. Katiyar and R. Uppaluri, *Int. J. Biol. Macromol.*, 2017, 94, 72–84.



Paper

- 20 L. Poon, S. Younus and L. D. Wilson, *J. Colloid Interface Sci.*, 2014, **420**, 136–144.
- 21 L. Poon, L. Wilson and J. Headley, *Carbohydr. Polym.*, 2014, **109**, 92–101.
- 22 C. Zhang, C. Shan, Y. Jin and M. Tong, *Chem. Eng. J.*, 2014, **254**, 340–348.
- 23 N. Sahiner, *Polymer*, 2017, **121**, 46–54.
- 24 Y. Yan, Q. An, Z. Xiao, W. Zheng and S. Zhai, *Chem. Eng. J.*, 2017, **313**, 475–486.
- 25 E. Platero, M. E. Fernandez, P. R. Bonelli and A. L. Cukierman, *J. Colloid Interface Sci.*, 2017, **491**, 1–12.
- 26 A. Hethnawi, N. N. Nassar, A. D. Manasrah and G. Vitale, *Chem. Eng. J.*, 2017, **320**, 389–404.
- 27 R. Shaimi and C. Low Siew, *J. Polym. Eng.*, 2016, **36**, 655.
- 28 Y. C. Xu, Z. X. Wang, X. Q. Cheng, Y. C. Xiao and L. Shao, *Chem. Eng. J.*, 2016, **303**, 555–564.
- 29 V. M. Boddu, K. Abburi, J. L. Talbott, E. D. Smith and R. Haasch, *Water Res.*, 2008, **42**, 633–642.
- 30 A. Sigdel, J. Park, H. Kwak and P.-K. Park, *J. Ind. Eng. Chem.*, 2016, **35**, 277–286.
- 31 R. Li, Q. Li, S. Gao and J. K. Shang, *Chem. Eng. J.*, 2012, **185–186**, 127–135.
- 32 K. R. Raj, A. Kardam and S. Srivastava, *Appl. Water Sci.*, 2013, **3**, 327–333.
- 33 S. Deng, G. Zhang, S. Chen, Y. Xue, Z. Du and P. Wang, *J. Mater. Chem. A*, 2016, **4**, 15851–15860.
- 34 N. Yaghi and H. Hartikainen, *APCBEE Proc.*, 2013, **5**, 76–81.
- 35 M. B. Shakoor, R. Nawaz, F. Hussain, M. Raza, S. Ali, M. Rizwan, S. E. Oh and S. Ahmad, *Sci. Total Environ.*, 2017, **601–602**, 756–769.
- 36 D. K. Singh, S. Mohan, V. Kumar and S. H. Hasan, *RSC Adv.*, 2016, **6**, 1218–1230.
- 37 B. A. Manning, S. E. Fendorf, B. Bostick and D. L. Suarez, *Environ. Sci. Technol.*, 2002, **36**(5), 976–981.
- 38 E. Guibal, *Sep. Purif. Technol.*, 2004, **38**(1), 43–74.
- 39 C. Daikopoulos, Y. Georgiou, A. B. Bourlinos, M. Baikousi, M. A. Karakassides, R. Zboril, T. Steriotis and Y. Deligiannakis, *Chem. Eng. J.*, 2014, **256**, 347–355.
- 40 J. K. Bediako, S. Lin, A. K. Sarkar, Y. Zhao, J.-W. Choi, M.-H. Song, W. Wei, D. H.-K. Reddy, C.-W. Cho and Y.-S. Yun, *J. Cleaner Prod.*, 2020, **252**, 119389.

